Hindawi
Advances in Physical Chemistry
Volume 2017, Article ID 4052373, 7 pages
https://doi.org/10.1155/2017/4052373

Research Article

Synthesis and Characterization of System In(O,OH)S/i-ZnO/n^+-ZnO

William Vallejo,[1] Carlos Diaz-Uribe,[1] and G. Gordillo[2]

[1]*Grupo de Fotoquímica y Fotobiología, Universidad del Atlántico, Km 7 Antigua vía Puerto Colombia, Barranquilla, Colombia*
[2]*Grupo de Investigación en Materiales Semiconductores y Energía Solar, Departamento de Física, Universidad Nacional de Colombia, Bogotá, Colombia*

Correspondence should be addressed to William Vallejo; williamvallejo@mail.uniatlantico.edu.co

Received 21 September 2016; Revised 18 January 2017; Accepted 1 February 2017; Published 15 March 2017

Academic Editor: Ali Eftekhari

In this work, we fabricated system In(O,OH)S/i-ZnO/n^+-ZnO to be used as potential optical window in thin films solar cells. i-ZnO/n^+-ZnO thin films were synthesized by reactive evaporation (RE) method and In(O,OH)S thin films were synthesized by chemical bath deposition (CBD) method; all thin films were deposited on soda lime glass substrates. Thin films were characterized through X-ray diffraction (XRD), atomic force microscopy (AFM), and spectral transmittance measurements. Structural results indicated that both thin films were polycrystalline; furthermore, morphological results indicated that both thin films coated uniformly soda lime glass substrate; besides, optical characterization indicated that system had more than 80% of visible radiation transmittance.

1. Introduction

Since their discovery, thin film solar cells have been considered a real option to compete with conventional silicon based solar cells; fewer amounts of chemical reagents and lower costs of manufacture than costs in silicon solar cells construction are main features of these devices. In last decades, research in this area was directed to study new ways to improve the efficiency of solar cells; currently, highest efficiency conversion reported to solar cells based on chalcopyrite absorbent layers (CIGS cell) is near to 21.0% ±0.6 (laboratory scale) [1].

General chalcopyrite-based solar cell structure is shown in Figure 1; in typical structure (known as substrate configuration) layers are deposited in sequence, molybdenum back contact, p-type CIGS absorber layer, n-type buffer layer, transparent conductor oxide (TCO), and top contact grid [2]. Inside absorbent layer, pairs of electron-hole are produced and light path and electron extraction from device rely on optical window (composed of buffer layer and TCO); buffer layer decreases the mechanical tension stress between absorbent layer and TCO electrode; besides, TCO is required for electron extraction from solar cells [3]. Usually, these devices use a CdS thin film as buffer layer in their structure; this layer improves mechanical heterojunction between absorbent layer and TCO; however CdS depicts environmental hazards during manufacture of the layers; besides, this material has a small forbidden energy band gap (E_g = 2.4 eV); this low-energy band gap reduces photocurrent at wavelengths near the ultraviolet region, and this incomplete absorption of the visible spectrum for CdS buffer layers is considered to be responsible for the drop in quantum efficiency of chalcopyrite-based solar cells [4–6]. Currently, deposition of Cd-free buffer layers without deteriorating stability of solar cell is an important research topic in the area. Best results of conversion efficiency are reported when buffer layers deposited by chemical bath deposition (CBD) are incorporated inside solar cells; this method is suitable for depositing uniform and adherent buffer layer in a large area; furthermore a variety of binary and ternary compounds can be sensitized by this way [7, 8]. Typical TCO as In_2O_3, SnO_2 F:SnO_2 and In:SnO_2, and

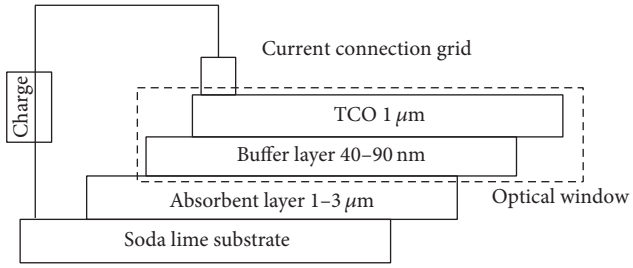

Figure 1: Typical structure to thin film solar cells.

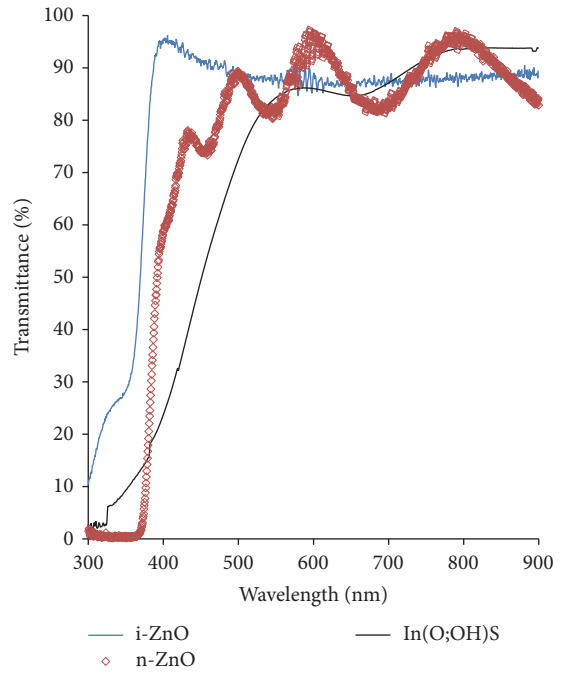

Figure 2: Optical transmittance to thin films deposited in this work.

ZnO are used in solar cell as electrical contact to extract electric power from solar cells [9–13]. Among these TCO's materials, Zinc Oxide (ZnO) has reported optimal results; it is a potential alternative to conventional indium-tin-oxide (ITO), which has been the most commonly TCO used in thin films solar cells [14, 15]. Different methods have been used to synthesize thin films of ZnO, such as spray pyrolysis [16], sputtering [17], MOCVD [18], and reactive evaporation (RE) [19]. Most of these methods reported transmittances near to 80% and low resistivity values at large range; however in most cases it is necessary to add dopants such as aluminum or indium to achieve suitable resistivity values. Different structures like ZnO/In_xSe_y and ZnO/ZnSe have been used as optical window in the fabrication of solar cells with structures $CuInSe_2$/In_xSe_y/ZnO and ZnO/ZnSe/CdTe, although best results were reported to CdS/In:SnO_3 system [20, 21].

In this paper we deposited In(O,OH)S thin films by the CBD method and i-ZnO/n^+-ZnO thin films by RE method. Results showed that system In(O,OH)S/i-ZnO/n^+-ZnO could be used as optical window to thin films solar cells.

2. Experimental

In this work we sensitized highly conductive and transparent thin films (n^+-ZnO, resistivity of 8×10^{-4} Ωcm) to be used as TCO in solar cells; furthermore we also deposited highly transparent and resistive thin films (i-ZnO, resistivity of 10^6 Ωcm) to be used as a diffusion barrier in solar cells; these thin films were deposited by RE in two-step process. The ionization of the reagent species was achieved through a low power glow discharge (GD) for applying a voltage of about 500 V-DC. Condition operations were as follows: glow discharge (2–20 mA), Zn temperature evaporation (470–510°C), partial pressure during GD (2×10^{-2}–5×10^{-2} mBar), and $O_{2(g)}$ flow (15–20 mLmin^{-1}) [22].

2.1. Buffer Layer Deposition. In this work, thin films of In(O;OH)S were deposited by CBD process for using reagents indium(III) chloride 2.5×10^{-2} M, thioacetamide 3.5×10^{-1} M, acetic acid 3.0×10^{-1} M, sodium citrate dihydrate 3.0×10^{-2} M, temperature at 70°C, and pH of 2.5. Thin films of In(O;OH)S were grown on soda lime (SL) substrates; chemical reaction can be written as follows:

$$\begin{aligned}&\left[\mathrm{In}\left(\mathrm{NH_3}\right)_{4-x}\mathrm{HCit}_x\right] + \mathrm{CH_3SCNH_2} + \mathrm{H3O^+}\\ &\longrightarrow \left[\mathrm{In\,(O;OH)\,S}\right]_{\mathrm{film}} + x\mathrm{HCit} + (4-x)\,\mathrm{NH_3}\\ &\quad + \mathrm{NCNH_2} + \mathrm{H_2O}\end{aligned} \tag{1}$$

After reaction synthesis, thin films were dried at ambient temperature under $N_{2(g)}$ stream.

2.2. Thin Films Characterization. The film thickness was measured through a Veeco Dektak 150 profilometer. The surface morphology of thin films was studied through PSI Microscope and atomic force microscopy (AFM). The optical properties of thin films were studied through transmittance measurements carried out with a Perkin Elmer Lambda 2S spectrophotometer. Finally, X-ray diffraction patterns of the samples were recorded in Shimadzu 6000 diffractometer with a source of Cu-K_α radiation (λ = 0.15418 nm) in a range diffraction angle 2θ between 20° and 80°. The electrical properties of TCO thin films were measured for using the four-probe method.

3. Results and Discussions

3.1. Optical Characterization. Optical transmittance of the thin films was studied from 300 nm to 900 nm of electromagnetic spectrum. Figure 2 shows the transmission spectra of In(O;OH)S (90 nm); these spectra show that buffer layer has optical transmission higher than 80% in the visible range and a sharp absorption edge at visible region; this result is typical to buffer layers and it is higher than typical transmittance of CdS thin films layers. Furthermore, Figure 2 also shows transmission spectra of i-ZnO (40 nm and resistivity of 10^6 Ωcm) and n^+-ZnO (900 nm and resistivity of 8×10^{-4} Ωcm) thin films; these spectra show that both i-ZnO and

n^+-ZnO have optical transmission between 80% and 90%, and the absorption coefficient was determined as follows:

$$\alpha(h\nu) = \frac{1}{d} \ln \frac{1}{T(h\nu)}, \quad (2)$$

where α is the absorption coefficient and d is the film thickness (obtained by profilometry). The optical energy band gap (E_g) of the films was determined using the relation:

$$(\alpha h\nu)^2 = A\left(h\nu - E_g\right), \quad (3)$$

where A is a constant depending on the transition probability; the optical band gap of the films was determined by extrapolating the linear portion of the $(\alpha h\nu)^2$ versus $h\nu$ plot on the x-axis [23–25]. Figure 3 shows E_g value to fitting equation (3). The band gap to buffer layer was In(O,OH),S (2.71 eV); this high value is due to CBD process; although CBD is a common fabrication process of thin films, most of reports did not explain mechanism of reaction; in literature two different processes are proposed to explain thin films formation: (a) homogeneous precipitation (HP): this mechanism is known as ion-by-ion precipitation; in this process thin films are generated by direct reaction of the ions under substrate surface; in first step free ions diffuse until substrate surface; after that, first nucleation centers of semiconductor are generated on substrate surface; after, nucleation center grows by addition of ions from solution; finally crystals grow and join other ones (coalescence process) and thin film of semiconductor is generated. (b) Heterogeneous precipitation (HeP): this mechanism is known as cluster-by-cluster precipitation; in this process thin films are generated by direct reaction of species into the reaction solution; in first step, colloidal particles are generated into solution (chalcogenide of metal or hydroxide of metal); after that, particles diffuse until substrate surface and first nucleation centers of semiconductor are generated on surface substrate; after that, nucleation center grows by addition of ions from solution. Finally crystals grow and join other ones (coalescence process) and thin film of semiconductor is generated [26, 27]. In CBD process both mechanisms can be present during thin films generation; the predominance of one mechanism to the other one will be determined by experimental condition (temperature, reagent concentration, pH, rate agitation, and complexing agents) [28]. The E_g value of In(O,OH)S is 2.71 eV; this value is greater than reported to In_2S_3; during synthesis process coprecipitation of other species and intermediates ($In(OH)_3$, In_2O_3) is common; in our case CBD process deposits In(O,OH)S; this result is confirmed by XRD results. Furthermore, band gap E_g of In(O,OH)S is greater than CdS (2.4 eV); this result is very positive due to the fact that blue response of device could be improved by the incorporation of this buffer layer [29].

Figure 3 also shows E_g to TCO; the main difference between the two types of films is observed in the interference patterns; i-ZnO thin film did not show pattern because of its reduced thickness (40 nm) and n^+-ZnO thin film shows typical interference patterns of this kind of layers.

The typical intrinsic defects in ZnO are the following: O vacancy (V_O), Zn vacancy (V_{Zn}), Zn interstitial (Zn_i), O interstitial (O_i), and antisite Zn (Zn_O). Zn interstitials and oxygen vacancies are known to be the predominant ionic defect types [26, 27, 30, 31]. This kind of defects can be controlled and we can obtain two types of ZnO conductivities; synthesis under excess of oxygen reduces V_O and synthesis under defect of oxygen increases V_O.

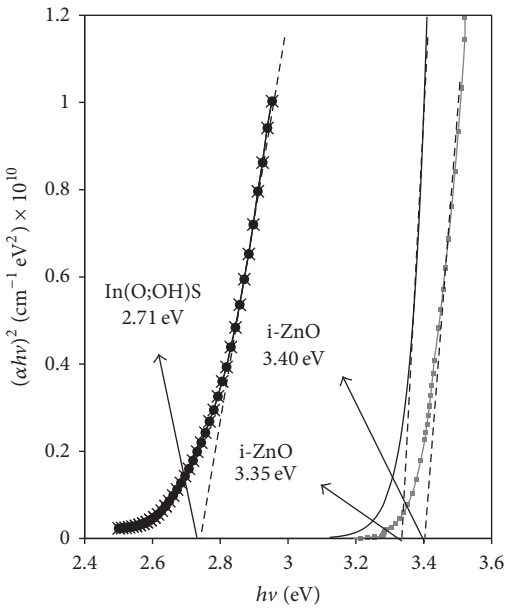

Figure 3: Linear fitting of $(\alpha h\nu)^2$ versus $h\nu$ plot (see (3)).

Figure 3 shows that n^+-ZnO thin film had an E_g value of 3.35 eV; besides, i-ZnO thin film had an E_g value of 3.40 eV; this value is according to other authors [32–36]. Optical results also show that i-ZnO antidiffusion layer does not affect transmittance of TCO; this is very important because this layer reduces species diffusion between heterojunctions to give chemical stability to solar cells on time. Finally, if we take into account only visible radiation (400 nm–750 nm) absorption effect, the optical window constructed in this work permits near to 83% of visible radiation reach to absorbent layer; results indicated that system In(O;OH)S/i-ZnO/n^+-ZnO has suitable optical properties to be used as optical window in thin film solar cells.

3.2. Structural Characterization. ZnO films were characterized through XRD measurements; Figure 4 shows experimental XRD patterns to i-ZnO and n^+-ZnO. Results show that the films of i-ZnO and n^+-ZnO have the same crystal structure corresponding to a hexagonal crystallographic structure (JCPDS # 36-1451); thin films had a preferential orientation in the plane of growth (002); this result is according to other reports [32, 33]. The signal intensity in n^+-ZnO thin film pattern is higher than to signal i-ZnO due to differences in the thickness of thin films. Furthermore, Figure 4 shows experimental XRD patterns to buffer layers. XRD pattern shows two signals located at $2\theta = 33.7^\circ$ and at $2\theta = 34.1^\circ$; these signals can be assigned to (001) and (200) planes from orthorhombic indium oxide hydroxide (InOOH) (JCPDS # 17-0549); third reflection is located at $2\theta = 48.37^\circ$;

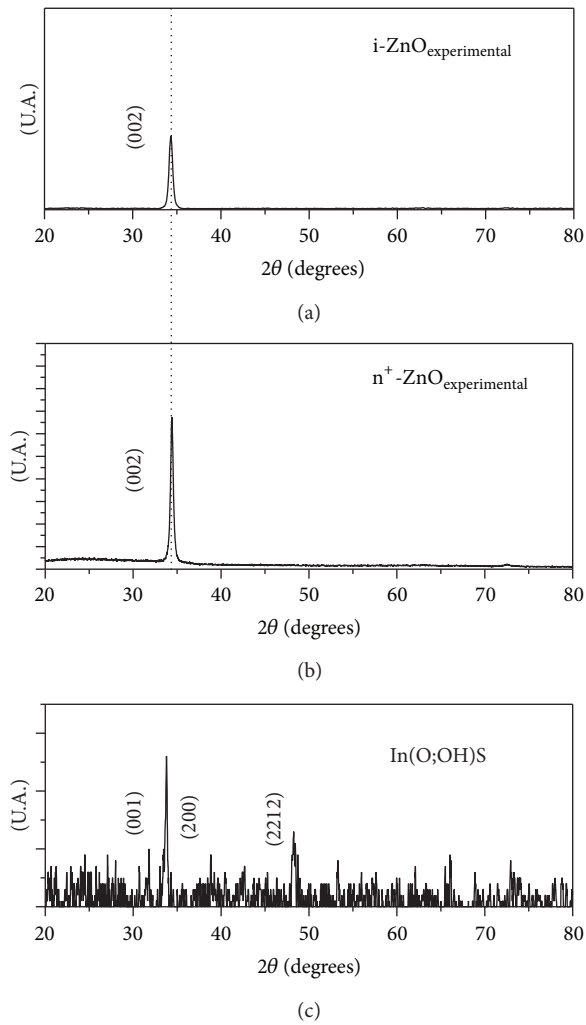

Figure 4: Experimental XRD patterns to (a) n$^+$-ZnO thin films, (b) i-ZnO thin films, and (c) In(O;OH)S thin films.

Table 1: Grain size average and roughness (Rms) values derived from images displayed in Figure 5.

Sample	Roughness Rms (nm)	Grain size (nm)
i-ZnO	4	60
n$^+$-ZnO	11	190
In(O;OH)S	7	90

this can be assigned to (2212) plane from tetragonal β-In_2S_3 phase (JCPDS #25-0390) [34, 35].

3.3. Morphological Characterization. Figure 5 shows AFM images of substrate and thin films deposited in this work; in Table 1 are listed the corresponding grain size average and roughness (Rms) values, which were determined through the ProScan image analysis software.

Figure 5(a) shows typical AFM image of soda lime glass (SLG) substrate; this figure shows a smooth surface and a reduced grain size (Table 1), typical values to SLG substrate. Figure 5 shows morphological changes after thin films deposition process; Figure 5(b) shows AFM image of In(O;OH)S thin film deposited by CBD on SLG substrate; Figure 5(b) shows crystalline grains that are well connected and they spread uniformly without any cracks; the image also shows crystallites are packed together; the average grain size of the films was near to 90 nm and roughness was 7 nm. Figures 5(c) and 5(d) show AFM images of n$^+$-ZnO and i-ZnO thin films deposited by RE on SLG. Results show that i-ZnO fill up uniformly SLG substrate; particles are distributed randomly throughout the SLG substrate without any crack. Furthermore, Figure 5(d) shows that the grain size and roughness of the films of n$^+$-ZnO are bigger than i-ZnO; this could be due to time used during synthesis process; time used in RE method is bigger to n$^+$-ZnO than i-ZnO. Finally, Figures 5(c) and 5(d) show that thin films are constituted by grains composed of crystallites with reduced size; these grains form a compact and uniform layer; when synthesis time increases are clear, those crystallites produced during first instants tend to form aggregates.

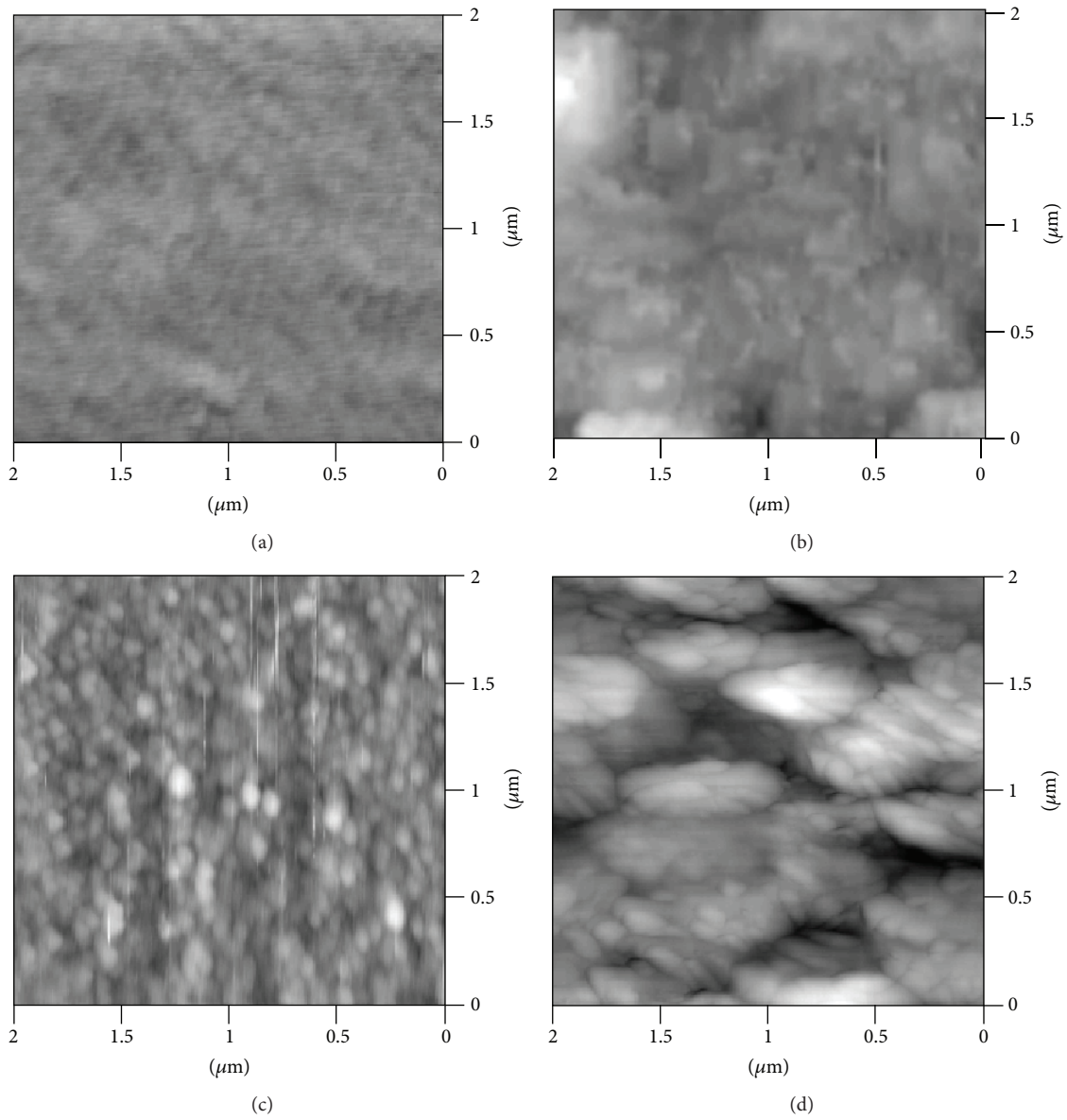

Figure 5: AFM images to (a) soda lime glass substrate, (b) In(O;OH)S thin films deposited by CBD on SLG, (c) i-ZnO thin films, and (d) n^+-ZnO thin films deposited by RE.

4. Conclusions

In this work we synthesized both thin films of ZnO and i-ZnO by RE method and thin films of In(O;OH)S by CBD method; optical results indicated that system ZnO/i-ZnO/In(O;OH)S had transmittance about 80% in visible region of electromagnetic spectrum. Furthermore, structural characterization indicated that TCO and buffer layer were polycrystalline; besides, morphological characterization indicated all thin films covered uniformly materials used as substrates. Finally, the antidiffusion layer could avoid migration of different chemical species through the heterojunction. Our results suggest that the system we proposed could be used as alternative optical windows in thin films solar cells.

Competing Interests

The authors declare that they have no competing interests.

Acknowledgments

This research was supported by Universidad del Atlántico (Project code CB20-FGI2016) and Universidad Nacional de Colombia.

References

[1] M. A. Green, K. Emery, Y. Hishikawa, W. Warta, and E. D. Dunlop, "Solar cell efficiency tables (version 47)," *Progress in*

Photovoltaics: Research and Applications, vol. 24, no. 1, pp. 3–11, 2016.

[2] R. W. Miles, "Photovoltaic solar cells: choice of materials and production methods," *Vacuum*, vol. 80, no. 10, pp. 1090–1097, 2006.

[3] J. L. Gray, "The physics of the solar cell," in *Handbook of Photovoltaic Science and Engineering*, A. Luque and S. Hegedus, Eds., p. 160, John Wiley & Sons, Chichester, UK, 2nd edition, 2010.

[4] N. Naghavi, G. Renou, V. Bockelee et al., "Chemical deposition methods for Cd-free buffer layers in CI(G)S solar cells: role of window layers," *Thin Solid Films*, vol. 519, no. 21, pp. 7600–7605, 2011.

[5] M. Nguyen, K. Ernits, K. F. Tai et al., "ZnS buffer layer for Cu2ZnSn(SSe)4 monograin layer solar cell," *Solar Energy*, vol. 111, pp. 344–349, 2015.

[6] D. H. Shin, J. H. Kim, S. T. Kim, L. Larina, E. A. Al-Ammar, and B. T. Ahn, "Growth of a High-quality Zn(S,O,OH) thin film via chemical bath deposition for Cd-free Cu(In,Ga)Se_2 solar cells," *Solar Energy Materials & Solar Cells*, vol. 116, pp. 76–82, 2013.

[7] S. Siebentritt, T. Kampschulte, A. Bauknecht et al., "Cd-free buffer layers for CIGS solar cells prepared by a dry process," *Solar Energy Materials and Solar Cells*, vol. 70, no. 4, pp. 447–457, 2002.

[8] D. Hariskos, S. Spiering, and M. Powalla, "Buffer layers in Cu(In,Ga)Se_2 solar cells and modules," *Thin Solid Films*, vol. 480-481, pp. 99–109, 2005.

[9] C. G. Granqvist, "Transparent conductors as solar energy materials: a panoramic review," *Solar Energy Materials and Solar Cells*, vol. 91, no. 17, pp. 1529–1598, 2007.

[10] J. Krc, B. Lipovsek, M. Bokalic et al., "Potential of thin-film silicon solar cells by using high haze TCO superstrates," *Thin Solid Films*, vol. 518, no. 11, pp. 3054–3058, 2010.

[11] C. Agashe, O. Kluth, G. Schöpe, H. Siekmann, J. Hüpkes, and B. Rech, "Optimization of the electrical properties of magnetron sputtered aluminum-doped zinc oxide films for opto-electronic applications," *Thin Solid Films*, vol. 442, no. 1-2, pp. 167–172, 2003.

[12] M. Berginski, J. Hüpkes, W. Reetz, B. Rech, and M. Wuttig, "Recent development on surface-textured ZnO:Al films prepared by sputtering for thin-film solar cell application," *Thin Solid Films*, vol. 516, no. 17, pp. 5836–5841, 2008.

[13] X.-L. Chen, J.-M. Liu, J. Ni, Y. Zhao, and X.-D. Zhang, "Wide-spectrum Mg and Ga co-doped ZnO TCO thin films for solar cells grown via magnetron sputtering with H_2 introduction," *Applied Surface Science*, vol. 328, pp. 193–197, 2015.

[14] A. Kassis and M. Saad, "Fill factor losses in ZnO/CdS/$CuGaSe_2$ single-crystal solar cells," *Solar Energy Materials and Solar Cells*, vol. 80, no. 4, pp. 491–499, 2003.

[15] J. B. Lee, H. J. Kim, S. G. Kim et al., "Deposition of ZnO thin films by magnetron sputtering for a film bulk acoustic resonator," *Thin Solid Films*, vol. 435, no. 1-2, pp. 179–185, 2003.

[16] E. Arca, K. Fleischer, and I. V. Shvets, "An alternative fluorine precursor for the synthesis of SnO_2:F by spray pyrolysis," *Thin Solid Films*, vol. 520, no. 6, pp. 1856–1861, 2012.

[17] M. H. Abdullah, L. N. Ismail, M. H. Mamat, M. Z. Musa, and M. Rusop, "Novel encapsulated ITO/arc-ZnO:TiO_2 antireflective passivating layer for TCO conducting substrate prepared by simultaneous radio frequency-magnetron sputtering," *Microelectronic Engineering*, vol. 108, pp. 138–144, 2013.

[18] M. L. Addonizio and L. Fusco, "Preparation method of double-textured ZnO:B films deposited by MOCVD on plasma etched polymer buffer," *Journal of Alloys and Compounds*, vol. 622, pp. 851–858, 2015.

[19] D. Yuvaraj and K. N. Rao, "Optical and electrical properties of ZnO films deposited by activated reactive evaporation," *Vacuum*, vol. 82, no. 11, pp. 1274–1279, 2008.

[20] G. Gordillo, "New materials used as optical window in thin film solar cells," *Surface Review and Letters*, vol. 9, no. 5-6, pp. 1675–1681, 2002.

[21] I. O. Oladeji, L. Chow, C. S. Ferekides, V. Viswanathan, and Z. Zhao, "Metal/CdTe/CdS/$Cd_{1-x}Zn_xS$/TCO/glass: a new CdTe thin film solar cell structure," *Solar Energy Materials and Solar Cells*, vol. 61, no. 2, pp. 203–211, 2000.

[22] J. S. Oyola, J. M. Castro, and G. Gordillo, "ZnO films grown using a novel procedure based on the reactive evaporation method," *Solar Energy Materials & Solar Cells*, vol. 102, pp. 137–141, 2012.

[23] J. Cheng, D. B. Fan, H. Wang, B. W. Liu, Y. C. Zhang, and H. Yan, "Chemical bath deposition of crystalline ZnS thin films," *Semiconductor Science and Technology*, vol. 18, no. 7, p. 676, 2003.

[24] W. T. Yen, Y. C. Lin, P. C. Yao, J. H. Ke, and Y. L. Chen, "Effect of post-annealing on the optoelectronic properties of ZnO:Ga films prepared by pulsed direct current magnetron sputtering," *Thin Solid Films*, vol. 518, no. 14, pp. 3882–3885, 2010.

[25] N. Revathi, P. Prathap, and K. T. R. Reddy, "Synthesis and physical behaviour of In_2S_3 films," *Applied Surface Science*, vol. 254, no. 16, pp. 5291–5298, 2008.

[26] A. F. Kohan, G. Ceder, D. Morgan, and C. G. Van De Walle, "First-principles study of native point defects in ZnO," *Physical Review B - Condensed Matter and Materials Physics*, vol. 61, no. 22, pp. 15019–15027, 2000.

[27] M. D. McCluskey and S. J. Jokela, "Defects in ZnO," *Journal of Applied Physics*, vol. 106, no. 7, Article ID 071101, 2009.

[28] G. Hodes, *Chemical Solution Deposition of Semiconductor Films*, Marcel Dekker, New York, NY, USA, 2002.

[29] M. A. Mughal, R. Engelken, and R. Sharma, "Progress in indium (III) sulfide (In_2S_3) buffer layer deposition techniques for CIS, CIGS, and CdTe-based thin film solar cells," *Solar Energy*, vol. 120, pp. 131–146, 2015.

[30] A. Janotti and C. G. Van de Walle, "Native point defects in ZnO," *Physical Review B*, vol. 76, no. 16, Article ID 165202, 2007.

[31] R. Vidya, P. Ravindran, H. Fjellvåg et al., "Energetics of intrinsic defects and their complexes in ZnO investigated by density functional calculations," *Physical Review B*, vol. 83, no. 4, Article ID 045206, 2011.

[32] B. Lin, Z. Fu, and Y. Jia, "Green luminescent center in undoped zinc oxide films deposited on silicon substrates," *Applied Physics Letters*, vol. 79, no. 7, pp. 943–945, 2001.

[33] J. C. Fan, K. M. Sreekanth, Z. Xie, S. L. Chang, and K. V. Rao, "P-Type ZnO materials: theory, growth, properties and devices," *Progress in Materials Science*, vol. 58, no. 6, pp. 874–985, 2013.

[34] P. F. Carcia, R. S. McLean, M. H. Reilly, and G. Nunes Jr., "Transparent ZnO thin-film transistor fabricated by rf magnetron sputtering," *Applied Physics Letters*, vol. 82, no. 7, pp. 1117–1119, 2003.

[35] D. J. Cohen, K. C. Ruthe, and S. A. Barnett, "Transparent conducting Zn1−xMgxO:(Al,In) thin films," *Journal of Applied Physics*, vol. 96, no. 1, pp. 459–467, 2004.

[36] C. Manoharan, G. Pavithra, S. Dhanapandian, P. Dhamodaran, and B. Shanthi, "Properties of spray pyrolised ZnO:Sn thin films and their antibacterial activity," *Spectrochimica Acta—Part A: Molecular and Biomolecular Spectroscopy*, vol. 141, pp. 292–299, 2015.